33rd Annual International Conference of the IEEE EMBS
Boston, Massachusetts USA, August 30 - September 3, 2011

Fundamental Sensing Limit of Electrochemical Glucose Sensors

Kevin Louchis and Stephen O'Driscoll, kdlouchis@ucdavis.edu and odriscoll@ucdavis.edu
Department of Electrical and Computer Engineering
University of California, Davis

***Abstract*—This paper investigates the inherent sensitivity limit, deactivation of glucose oxidase, of a glucose oxidase based electrochemical glucose sensor for in vivo monitoring of blood glucose concentration. Results in this paper show that the current density sensitivity to glucose decreases from $1200nA/mm^2/mM$ at initial implantation to $100nA/mm^2/mM$ after an implantation time of 2 years, when degradation due to glucose oxidase deactivation only is considered. Even as the sensor signal strength decreases, if the sensing electronics are sufficiently discriminating then a useful measure of blood glucose concentration can be extracted. This work aims to determine both how the glucose oxidase based sensor's signal-to-noise ratio degrades over long time scales and the electronic circuit requirements to achieve multi-year device lifetimes. Two sensing amplifier techniques are presented which can be used to detect the signal generated by the sensor. The noise performance of each technique is compared with the noise performance of the sensor and mutli-year lifetimes are shown to be feasible.**

I. Introduction

Diabetes can produce severe health problems, but these can be reduced by a factor between 21% to 63% with continuous monitoring of a patient's blood glucose concentration [1]. An autonomous sensor that can be implanted into the body would allow the continuous, seamless monitoring of a patient's blood glucose concentration. This work investigates the fundamental lifetime limit of an electrochemical glucose sensor and design considerations for the acquisition of the glucose signal. This work aims to determine both how the glucose oxidase based sensor's signal-to-noise ratio degrades over long time scales and the electronic circuit requirements to achieve multi-year device lifetimes. Such extended lifetimes of the sensor are essential for implantable glucose sensors for continuous monitoriting to be feasible.

The electrochemical glucose sensor has an enzyme immobilized on its surface which reacts with glucose to produce an electric current that is a function of the concentration of glucose. Recent work in developing implantable electrochemical glucose sensors [2], [3] is encouraging. Nevertheless, several issues limit the lifetime of the sensor to only a few months [4]: biological imperfections in the implantation cavity; the concentration of oxygen available to the sensor; bacterial growth on the sensor; clogging at the sensor interface; and degradation of the enzyme that reacts with glucose. However enzyme deactivation represents an inherent performance limit. Even if improved package design reduces the effect of the other non-idealites, the performance of the sensor will not surpass the inherent limit caused by enzyme deactivation. Therefore this initial investigation focuses on modeling the degradation of the sensor output due to sensor enzyme deactivation over time and determines the required circuit performance to extract a useful signal from the degraded output after five years, and presents circuits to achieve that performance. Future work will incorporate other non-ideal factors such as implantation imperfections, bacterial growth, sensor clogging, and interfering molecules in our sensor model.

II. Glucose Oxidase Sensor

A. Typical Device Layout

A conceptual view of a typical electrochemical sensor is shown in Fig. 1. The electrochemical sensor (ECS) consists of three electrodes: the working electrode (WE), reference electrode (RE), and counter electrode (CE). The integrated circuit shown in Fig. 1 will contain a bias circuit to properly bias the sensor's electrodes and a sensor amplifier to amplify the signal generated by the ECS.

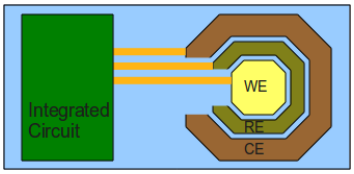

Fig. 1. Conceptual view of a typical glucose oxidase based electrochemical sensor system showing the integrated circuit as well as the working, reference, and counter electrodes (labeled WE, RE, and CE respectively).

The WE has glucose oxidase (GOD) immobilized on its surface, as glucose reacts with the GOD a current is generated that is a function of the glucose concentration at the WE. The RE is used to apply a biasing potential between the WE to the RE. The CE is used to sink the current created by the chemical reactions at the surface of the WE by sourcing electrons to the WE.

B. Chemical Model

The reduction and oxidation (redox) reactions that occur between the glucose molecules and the GOD molecules is described in Eqs. (1) and (2) [5].

$$E_{ox} + G \xrightarrow{k_1} E_{ox}G \xrightarrow{k_2} E_{red} + \delta lactone \quad (1)$$

$$E_{red} + O_2 \xrightarrow{k_4} E_{ox} + H_2O_2 + 2e^- \quad (2)$$

Over time GOD molecules react with the H_2O_2 produced by the redox reaction. The reaction between GOD and H_2O_2 causes the GOD to be irreversibly deactivated. The chemical model of this deactivation is shown in Eqs. (3), (4), and (5).

$$E_{ox} + H_2O_2 \xrightarrow{k_d^{(1)}} E_i^{(1)} \tag{3}$$

$$E_{ox}G + H_2O_2 \xrightarrow{k_d^{(2)}} E_i^{(2)} \tag{4}$$

$$E_{red} + H_2O_2 \xrightarrow{k_d^{(3)}} E_i^{(3)} \tag{5}$$

Where G represents glucose, E_{ox} represents the oxidized form of GOD, E_{red} represents the reduced form of GOD, $E_{ox}G$ represents an intermediate state of GOD while it is bonded with the glucose, and $E_i^{(n)}$ is the n^{th} irreversibly deactivated state of GOD. The value k_2 is a first order reaction rate coefficient (in units of $M^{-1}s^{-1}$) and the values k_1, k_4, $k_d^{(1)}$, $k_d^{(2)}$, $k_d^{(3)}$ are second order reaction rate coefficients (in units of s^{-1}). These equations show that the redox reaction is not only dependent on the concentration of glucose at the WE, but also on the concentration of oxygen. Reactions in Eqs. (1) and (2) produce δ-lactone and H_2O_2. The total redox reaction including deactivation is graphically represented in the state diagram shown in Fig. 2. The lines connecting each state of GOD represents a transition in the chemical reactions in Eq. (1)-(5). The quantities along each line represent that particular reaction rate (in units of M/s). That is to say the rate of change of the concentration of E_{ox} can be found by summing each line connected the E_{ox} state, this is shown in Eq. (6). Similar rate equations can be obtained for each state.

$$\frac{d[E_{ox}]}{dt} = k_4[E_{red}][O_2] - k_1[E_{ox}][G] - k_d^{(1)}[E_{ox}][H_2O_2] \tag{6}$$

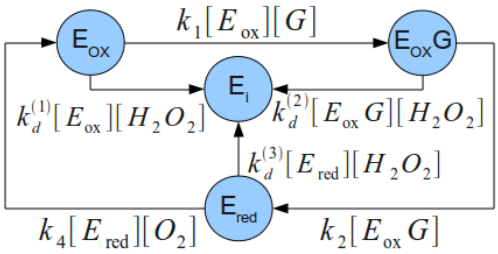

Fig. 2. State diagram showing the rates at which glucose oxidase changes through the three redox states and into the permanently inactive state.

As shown in Eq. (2) each redox reaction releases two free electrons that contribute to the current that is a function of the concentration of glucose. The average current produced by the sum of all the redox reactions is defined in Eq. (7) [6].

$$i_{ox} = FA_{WE}[E_{ox}]\sqrt{D_{GE}k_f} \tag{7}$$

In Eq. (7) i_{ox} is the average current produced by the sensor as a result of redox reactions (redox current), F is Faraday's Constant, A_{WE} is the area of the WE, $[E_{ox}]$ is the concentration of oxidized GOD, D_{GE} is the diffusion coefficient of glucose in the enzyme layer of the working electrode, and k_f is the oxidation reaction rate.

The relationship between the concentration of glucose and the concentration of the oxidized state of GOD can be solved numerically by integrating the differential equations that model the redox reaction. One such differential equation is shown in Eq. (6).

C. Electrical Model

The redox current at the WE is very weak, typically on the order of μA's after initial implantation, therefore it is first amplified. To better understand the requirements of the sensing amplifier, an electrical model of the sensor is required. The electrical model of an ECS as presented in [3] is used, as shown in Fig. 3.

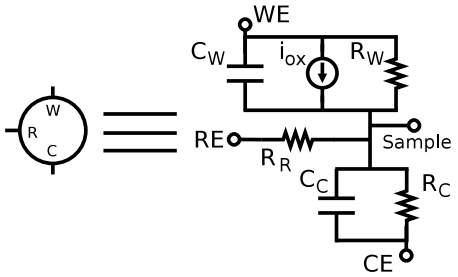

Fig. 3. Electrical model of electrochemical glucose sensor with equivalent three terminal model.

Where i_{ox} is the oxidation current modeled in Eq. (7), R_W and C_W are the WE resistance and capacitance, R_C and C_C are the CE resistance and capacitance, and R_R is the RE resistance. Not shown in the model is the noise current generated by the electrode to electrolyte interface between the working electrode and the solution. The noise power spectral density (PSD) generated at the interface between the WE and the sample, $G_{i_{WE}}$, is expressed in Eq. (8) [7]. Also not modeled in the Fig. 3 are the thermal noise current sources in parallel with the electrode resistances represented by the PSDs $G_{i_{R_W}}$, $G_{i_{R_R}}$, and $G_{i_{R_C}}$.

$$G_{i_{WE}} = 2qi_{ox} \tag{8}$$

III. Transimpedance Amplifier

The oxidation current, i_{ox}, is very weak and must be amplified before further processing. A transimpedance amplifier (TIA) is typically used to convert the small current to a large voltage. The two TIA techniques most commonly used in glucose sensors are presented and their noise performance is analyzed and compared to that of the ECS.

A. Operational Amplifier with Shunt Feedback

The system level schematic of the op amp with shunt feedback TIA is shown in Fig. 4.

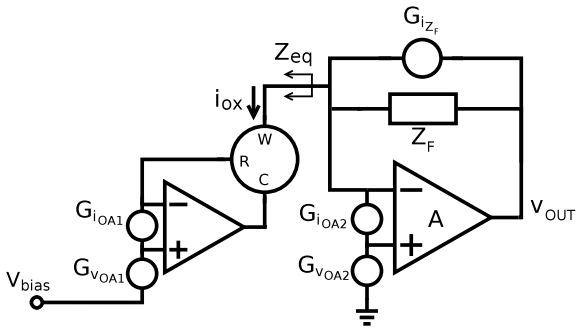

Fig. 4. System level model of a TIA consisting of an op amp with shunt feedback Z_F. Noise sources for noise contributing elements are included.

The small signal transimpedance of the shunt feedback TIA is given by Eq. (9).

$$\frac{v_{out}}{i_{ox}} = \frac{-A}{\frac{1}{Z_{eq}} + \frac{A+1}{Z_F}} \tag{9}$$

Where Z_{eq} is the impedance seen looking towards the ECS as shown in Fig. 4. The impedance Z_{eq} is defined in Eq. (10).

$$Z_{eq}(\omega) = \frac{R_W}{1 + j\omega R_W C_W} + \frac{R_C}{(A+1)(1 + j\omega R_C C_C)} \tag{10}$$

The noise characteristics of this TIA can be analyzed by considering power spectral densities (PSDs) $G_{i_{OA}}$ and $G_{v_{OA}}$ due to the op amp, and $G_{i_{Z_F}}$ due to feedback impedance Z_F. The equivalent PSD of the total noise referred to the redox current i_{ox} is given in Eq. (11).

$$\begin{aligned} G_{i_{ox}}|_{TIA} =& (G_{i_{OA}} + G_{i_{Z_F}}) \left| \frac{Z_F}{(A+1)Z_{eq}} \right|^2 \\ &+ G_{v_{OA}} \left| \frac{A}{(A+1)Z_{eq}} \right|^2 \end{aligned} \tag{11}$$

The noise generated by the sensor and its bias circuit can also be referred to the redox current to be compared with the noise of the TIA. This noise is given in Eq. (12), which is valid assuming that $A \gg 1$.

$$\begin{aligned} G_{i_{ox}}|_{SENSOR} \approx & G_{v_{OA}} \left| \frac{1}{Z_W} \right|^2 + G_{i_{OA}} \left| \frac{R_R}{Z_W} \right|^2 + G_{i_W} \\ &+ G_{i_C} \left| \frac{Z_C}{Z_W} \right|^2 + G_{i_R} \left| \frac{R_R}{Z_W} \right|^2 + G_{i_{WE}} \end{aligned} \tag{12}$$

Where Z_W represents the parallel combination of C_W and R_W, and Z_C represents the parallel combination of C_C and R_C.

B. ECS integrated with TIA

A circuit diagram of the TIA integrated with the ECS is shown in Fig. 5. The small signal transimpedance of this TIA is given by Eq. (13).

$$\frac{v_o}{i_{ox}} = \frac{1}{g_m} \tag{13}$$

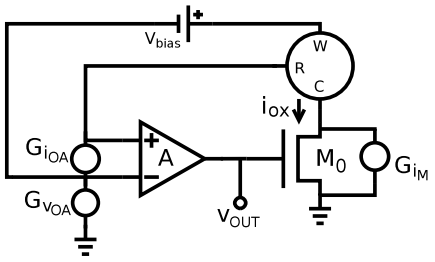

Fig. 5. Circuit model of the TIA integrated with the ECS bias circuit. Noise sources for for noise contributing elements are included.

The noise characteristics of this TIA can be analyzed by considering PSDs $G_{i_{OA}}$ and $G_{v_{OA}}$ due to the op amp, and G_{i_M} due to transistor M. The PSD of the noise referred to the redox current i_{ox} is given in Eq. (14).

$$\begin{aligned} G_{i_{ox}}|_{TIA} = G_{i_{OA}} (1 + A g_m R_R)^2 + & G_{v_{OA}} (A g_m)^2 \\ & + G_{i_M} \end{aligned} \tag{14}$$

The noise generated by the sensor can also be referred to the redox current to be compared with the noise of the TIA. This noise is given in Eq. (15).

$$G_{i_{ox}}|_{SENSOR} = G_{i_W} + G_{i_R}(g_m A R_R)^2 + G_{i_{WE}} \tag{15}$$

C. Quantitative Comparison

The two TIA configurations presented have different noise characteristics when referring the system noise to the oxidation current, i_{ox}. The feedback TIA takes its input from the WE, and the large WE impedance ($\sim$ 10MΩ at DC [3]) attenuates the noise from the sensor and bias circuit. The integrated TIA takes its input from the CE, and the large WE impedance does not decease the sensor noise. The larger noise contribution from the ECS causes the integrated TIA to have a greater overall noise than the feedback TIA. This affects the lifetime of the sensor as the signal strength will fall below the noise level earlier. However, the integrated TIA contains only one op amp and uses a transistor rather than a resistor in feedback whereas the feedback TIA requires a second op amp to bias the ECS. This allows the integrated TIA to use less power than the feedback TIA to achieve the same transimpedance gain but at a higher noise cost.

IV. Simulations

To compare the TIA techniques, the noise PSD referred to i_{ox} was simulated for circuits with typical values. All op amps are simulated as an ideal op amp with finite gain of 10000, an input referred noise voltage and current spectral density of $1\times10^{-18}V^2/Hz$ and $1\times10^{-24}A^2/Hz$ (typical values for low noise CMOS amplifiers). The feedback transistor M_0 in the integrated TIA has a small signal transconductance of $7\mu A/V$ and a drain current noise PSD density of $3.5\times10^{-26}A^2/Hz$. The feedback impedance used in the feedback TIA has a value of $140k\Omega$, this was chosen so the transimpedance gain of both TIAs would match. For the feedback TIA, the TIA contribution to the PSD referred to i_{ox} is $2\times10^{-24}A^2/Hz$,

while the sensor's contribution to the PSD referred to i_{ox} is $3 \times 10^{-26} A^2/Hz$, for frequencies below 100kHz. For the integrated TIA, the TIA contribution to the PSD referred to i_{ox} is $4.9 \times 10^{-19} A^2/Hz$, while the sensor's contribution to the PSD referred to i_{ox} is $3.85 \times 10^{-19} A^2/Hz$, for frequencies below 100kHz.

The relationship between the concentration of glucose at the surface of the WE and the redox current produced by the sensor can be solved for numerically by arranging the chemical equations (1)-(5) into differential equations as shown in Eq. (6). Using numerical integration, the sensitivity of the sensor was simulated. Fig. 6 shows the simulation results. The sensitivity of the sensor is defined as the current density per unit concentration of glucose.

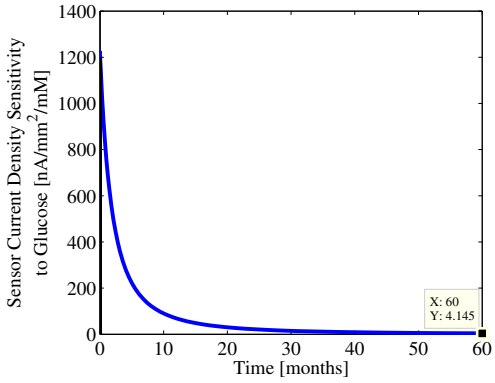

Fig. 6. Simulated results of the sensor's sensitivity to glucose over five years with a GOD concentration of $25mM$ at the WE when the sensor is exposed to a sample with an oxygen concentration of $25mM$.

To find when the current output of the ECS is less than the rms noise referred to i_{ox} the PSDs can be integrated to a certain noise bandwidth to find the rms value of the noise within that bandwidth. Fig. 7 shows the rms values of each TIA integrated to a bandwidth of 10kHz. The redox currents over time for $1mm^2$, $0.5mm^2$, and $0.1mm^2$ WEs with the same oxygen and GOD concentration are shown Fig. 7.

Fig. 7 shows that after about 27 months the feedback TIA rms noise will be greater than the redox current of the ECS, even for the $1mm^2$ WE. The integrated TIA has an rms noise less than the redox current even after 60 months for a $1mm^2$ WE. Using the simulation results presented, the point in time where the rms noise generated by the TIA will become greater than the redox current of the ECS can be found. This point in time is the fundamental lifetime limit of the ECS. However, the real lifetime of the sensor will be less as there are other means of sensor redox current degradation in addition to GOD deactivation.

V. Conclusion

The concentration of glucose oxidase available to react with glucose decreases over time. This deactivation establishes a fundamental limit on the lifetime of the sensor. Two transimpedance amplifiers which acquire the redox signal and convert and amplify it into a voltage have been presented. The noise generated by the transimpedance amplifier has been referred to the redox current at the working electrode. Once the redox current from the electrochemical sensor degrades below the in band the total system noise referred to the redox current then the transimpedance amplifier will no longer be able to acquire the signal. This initial work demonstrates that, given current circuit technology, the fundamental limit of the lifetime of electrochemical glucose sensing, i.e. that due to glucose oxidase deactivation, exceeds five years for practical implantable sensor sizes. Future work will model additional material-related limitations such as bacterial growth in the vicinity of the electrodes; interfering molecules; and clogging effects.

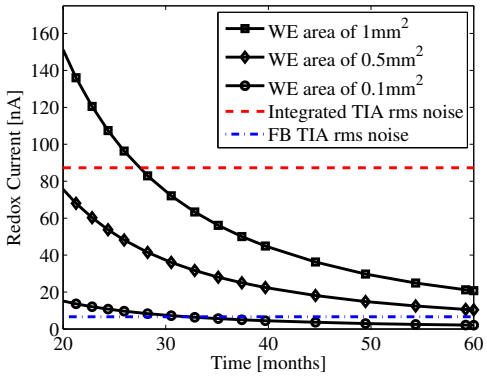

Fig. 7. Signal strength of a $1mm^2$ WE ECS over time with rms redox referred noise currents for a feedback TIA and an integrated TIA.

References

[1] UKPDS, "Intensive blood-glucose control with sulphonylureas or insulin compared with conventional treatment and risk of complications in patients with type 2 diabetes (UKPDS 33). UK Prospective Diabetes Study (UKPDS) Group.," *Lancet*, vol. 352, pp. 837–53, Sept. 1998.

[2] M. Ahmadi and G. Jullien, "A wireless implantable microsystem for continuous blood glucose monitoring," *IEEE Transactions on Biomedical Circuits and Systems*, vol. 3, no. 3, pp. 169–180, 2007.

[3] S. M. Martin, F. H. Gebara, T. D. Strong, and R. B. Brown, "A Fully Differential Potentiostat," *IEEE Sensors Journal*, vol. 9, pp. 135–142, Feb. 2009.

[4] G. Reach and G. S. Wilson, "Can continuous glucose monitoring be used for the treatment of diabetes?," *Analytical Chemistry*, vol. 64, pp. 381A–386A, Mar. 1992.

[5] C. O. Malikkides and R. H. Weiland, "On the mechanism of immobilized glucose oxidase deactivation by hydrogen peroxide.," *Biotechnology and bioengineering*, vol. 24, pp. 2419–39, Nov. 1982.

[6] R. S. Nicholson and I. Shain, "Theory of Stationary Electrode Polarography," *Analytical Chemistry*, vol. 36, no. 4, pp. 706–723, 1964.

[7] A. Hassibi, R. Navid, R. W. Dutton, and T. H. Lee, "Comprehensive study of noise processes in electrode electrolyte interfaces," *Journal of Applied Physics*, vol. 96, no. 2, p. 1074, 2004.